

# Effects of Electrostatic Polarity and the Types of Electrical Charging on Electrospinning Behavior

Chang-Mou Wu,<sup>1</sup> Hau-Geng Chiou,<sup>1</sup> Siang-Ling Lin,<sup>1</sup> Jian-Min Lin<sup>2</sup>

<sup>1</sup>Department of Fiber and Composite Materials, Feng Chia University, Taichung, Taiwan 40724, Republic of China

<sup>2</sup>Department of Products, Taiwan Textile Research Institute, Tucheng, New Taipei, Taiwan 23674, Republic of China

Received 4 July 2011; accepted 20 December 2011

DOI 10.1002/app.36680

Published online in Wiley Online Library (wileyonlinelibrary.com).

**ABSTRACT:** In this study, we examined the effect of applied electrostatic voltages and the types of electrical charging on jet movement, fiber productivity, fiber diameter and deposited configuration by two inverse polarity systems, termed as spinneret and collector charging systems. Jet movement parameters such as Taylor cone, straight jet length, whipping angle, and pitch of whipping loop are examined and compared. The results show that the electronegative collector charging system or the electropositive spinneret charging system is superior to their contrastive system in terms of smaller fiber diameter, compact fiber deposited configuration, and higher fiber productivity. Optimal applied voltage found was 25 kV for electronegative collector charging system and 30 kV for electropositive spinneret charging system and resulted in

finest fiber diameter (209 nm for electronegative collector charging system and 247 nm for electropositive spinneret charging system). Polyvinyl acetate solution jet is easier to be ejected, stretched, and accelerated under electropositive charging. The spinning jet with electropositive charges can be achieved either in the spinneret charging system by using electropositive charger or in the collector charging system by using electronegative charger. This finding is an important guideline for the designing of electrospinning device. © 2012 Wiley Periodicals, Inc. *J Appl Polym Sci* 000: 000–000, 2012

**Key words:** processing; nanofiber; solution properties; electrospinning behavior; electrostatic polarity

## INTRODUCTION

Electrospinning technology, introduced by Formhals et al. in 1934,<sup>1</sup> is a manufacturing technique that extracts continuous nanofibers from polymer solution or melts under a strong electrostatic field. By adjusting polymer solution types and manufacturing parameters, the produced fibers can range in diameter from several micrometers to several tens of nanometers. In fact, not all polymer solutions can form electrospinning jet under an electrostatic field. As far as the polymer solution properties are concerned, viscosity plays a dominant role in electrospinning process. The prerequisite for fiber formation during electrospinning is the presence of sufficient cohesive force in the working solution to develop a deformable entangled chain structure, and therefore preventing jet breakup.<sup>2</sup> Fiber manufactured using this method possesses several

attractive characters such as small diameter, high specific surface area, flexibility in surface functionalities, high porosity, and so on. Thus, the nanofibers can be used as filter material, biomedical element, tissue scaffolds, biosensors, photoelectric components, reinforced composite materials, and so on.<sup>3–7</sup>

Electrospinning is a special form of polymeric fluid electrostatic atomization.<sup>8</sup> The primary difference is that instead of droplets, an extended jet flow is obtained. The jet flow can extend to a long distance, thereby obtaining a superfine fiber. Theoretical analysis of electrospinning is extremely complicated, involving fields in physical and chemical engineering, mainly subjects such as electrostatics, electrohydrodynamics, rheology, aerodynamics, charge transfer between solid and liquid surfaces, mass transfer, heat transfer, and so on. In the electrospinning system, charge accumulates on the surface of the spinning solution owing to electrostatic field effects. The dynamic effects of the surface tension, viscoelastic forces of the spinning solution, and distribution of the charge (Coulomb forces) on the surface play an important role in the process of electrospinning.<sup>9,10</sup>

Typical electrospinning process can be divided into four regions: base, jet, whipping, and collection.<sup>11</sup> The electrospinning activity starts from the base.

Correspondence to: C.-M. Wu (cmwu@fcu.edu.tw).

Contract grant sponsor: National Science Council of Taiwan; contract grant number: NSC100-2221-E-035-028.

Contract grant sponsor: Taiwan Textile Research Institute.

When external voltage reaches critical voltage, the semi-spherical liquid drop becomes conical and forms jet which is ejected from the tip of the cone and flows toward the collector. The resulting cone shape is known as the Taylor cone.<sup>12</sup> The critical voltage is related to the distance between the spinneret tip and the collector, the spinneret length, the spinneret radius, and the surface tension of the electrospinning solution.<sup>13,14</sup> Spinning solution at the spinneret tip forms Taylor cone owing to the interactions of surface tension, electrostatic field force, viscosity, and Coulomb forces.<sup>4,15,16</sup> Jet is a region between the base and the whipping region. In this region, the electrostatic forces continue to accelerate and stretch the jet flow and it causes decreasing of fiber diameter. This region is mainly affected by the electrostatic field forces and viscosity of the stretching jet. The combined force of the two becomes a longitudinal stretching force that contributes to the steady linear movement of the jet. The distance of the jet flow is called the straight jet length.<sup>17</sup> During jetting process, the viscous resistance prevents the jet from moving forward, as a result the acceleration becomes smaller and smaller. When the jet encounters small perturbation, its straight movement will destroy, and whipping instability occurs.<sup>17</sup> The jet rotates into a complex conical path with its vertex at the end of the straight segment. By observing images obtained using a high-speed camera, Shin et al.<sup>18</sup> showed that the inverted conical body is actually an image formed by the rapid and unstable whipping of a single jet. Surface tension counteracts the whipping instability because whipping always causes an increase of the jet surface area. If the jet did not whip, much kinetic energy would be required to keep the leading part ahead of the following parts of the jet. By whipping, the electrical energy supplied to the jet was instead used efficiently to elongate the jet, decrease its diameter, and thereby produce more surface area per unit mass of fluid. Thus, the onset of whipping instability indicates the onset of rapidly increasing surface area. Evaporation of the solvent changes the viscoelastic properties of the polymer solution and stops the elongation. This region between the jet and the collection is referred as whipping region, which is the primary cause for the rapid decrease of the fiber diameter and the large stretch ratio obtained in electrospun nanofibers. The collection region is where jet activities stop. When solvents evaporate and solutes solidify, the resulting fiber will deposit on the collector. The composition of the collector, as well as the type of the electrostatic field, greatly influences the jet movement and the fiber configuration.

Surveying literature on electrospinning, there are several articles reported on the development and modification of electrospinning devices. An electrospinning device is mainly composed of electrostatic controller, spinneret, collector, and injection pump.

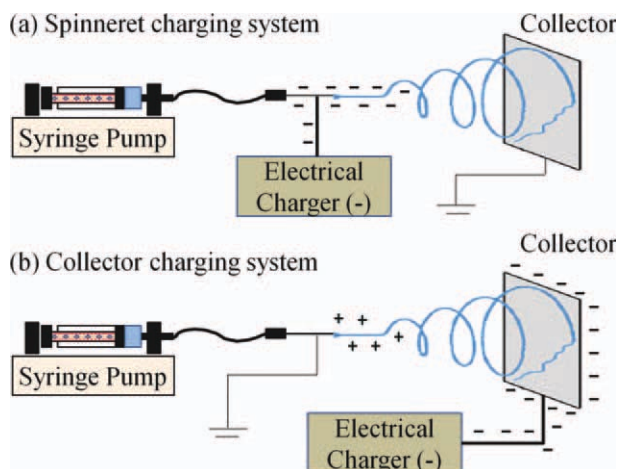
Methods of increasing the productivity of the nanofibers are reported as multiple-spinning setup<sup>19–22</sup> and needleless electrospinning.<sup>23</sup> In addition, many studies focus their research on the collector modification for obtaining aligned, patterned nanofiber, or fiber yarn. To accelerate the spinning jet or to orient the fibers, these studies either applied extra electrostatic fields in the electrospinning device or changed the gathering equipment to alter the path of jet movement. The implemented techniques reported such as rotating cylinder,<sup>24,25</sup> wire drum,<sup>26</sup> tapered wheel-like bobbin,<sup>27–29</sup> auxiliary electrode,<sup>30–33</sup> electric field,<sup>34</sup> and so on. It is worthy to note that most electrospinning devices connect high-voltage electrostatic to the spinneret and change the processing parameters (such as voltage, working distance, solution flowing speed, spinneret diameter, etc.) or solution parameters (such as viscosity, concentration, molecular weight, and conductivity) to study the relationship between the parameters and the fiber configuration. Kilic et al.<sup>35</sup> first reported the effects of polarity on electrospinning and compared electrospinning efficiency and fiber morphologies in two charging systems. In the first system, the spinneret was charged by direct current, positive electricity power supply, and the collector served as ground. In the other system, the placement of charge and ground was reversed. Their results indicated that the spinneret charging system was better than the other under the same parameters. However, as indicated above, electrostatic fields applied on the spinneret or the collector definitely change the electrospinning behavior and fiber configuration. The optimal electrospinning parameters for the two systems must be different and have to be studied in more detail.

Fully aware of the significant influence of polarity on electrospinning process, it is important to examine electrostatic polarity and the types of electrical charging on the electrospinning jet movement, productivity, fiber diameter, and deposited configuration. Two inversely electrospinning charging systems, termed as spinneret charging and collector charging systems, were used for the electrospinning behavior study. Jet movement parameters such as the Taylor cone, straight jet length, whipping angle, and pitch of whipping loop are examined and compared. It is believed that an understanding on the effect of polarity and the types of electrical charging on the electrospinning behavior shall provide valuable information for guiding the designing of electrospinning device.

## EXPERIMENTAL

### Material

Polyvinyl acetate (PVA, Sigma-Aldrich): 98–99% hydrolyzed, with a molecular weight of 146,000–



**Figure 1** Schematic diagram of two electrospinning apparatus (a) spinneret charging system and (b) collector charging system (Electronegative charger). [Color figure can be viewed in the online issue, which is available at [wileyonlinelibrary.com](http://wileyonlinelibrary.com).]

186,000 was used in this study as received. The concentration of the prepared PVA aqueous solution was 7 wt %. The measured viscosity is 383 mPa s which was determined by a rotary viscometer (LVDVII+, Brookfield, WI) at 30°C.

### Electrospinning

The electrospinning device consists of an injection spinneret connected to a syringe pump (KDS 101, Kd Scientific, Holliston, MA USA). The syringe pump was connected to a Teflon tube which was attached to a stainless steel needle with 0.31-mm internal diameter acting as a spinneret. A copper grid covered by construction paper acted as the collector. The working distance was kept at 18 cm from the needle to the collector and flow rate was maintained as 0.008 mL/min for all the experiments. An electrostatic controller (LGC-300, Taiwell, Taiwan) connected to the spinneret and the collector was grounded as shown in Figure 1(a), which was referred as spinneret charging system. Alternatively, a charged collector and grounded spinneret, as shown in Figure 1(b), was referred as the collector charging system. The applied voltage for electrospinning process was systematically varied from 5 to 40 kV at 40% relative humidity (RH). A typical jet movement image is shown in Figure 2 in which jet parameters such as the Taylor cone, the straight jet length, whipping angle, and pitch of whipping loop are indicated.

### Characterization

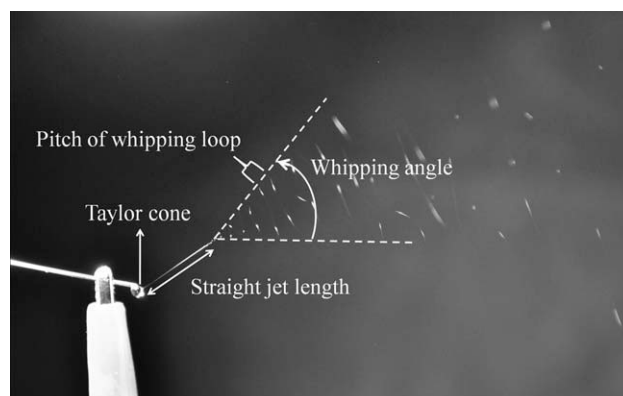
The distances for straight jet length, whipping angle, and pitch of whipping loop were measured man-

ually from the optical digital images. A stroboscope (DS-3200, SAGA, USA) was added for a better observation on the jet motion and to enhance the resolution of optical images. The distance was determined by using Motic Images Plus 2.0 ML software (Motic®, Xiamen, China). Scale was determined according to the outer diameter of the spinneret (0.55 mm). A variable vacuum scanning electron microscope (S3000, Hitachi, Japan) and an optical microscope (BHZ-UMA, Olympus, Japan) were used to observe the deposited fiber configurations, fiber diameters, and the fiber morphology. The thickness of deposited nanofiber web was measured using a stylus contact type surface profilometer (ET-3000, Kosaka Laboratory, Japan). Diamond-tipped stylus was used for thickness measurement in direct contact and scanned across the sample surface. Part of the deposited nanofiber web was mechanically removed to make a step, and the stylus scanned throughout the step. The thickness was determined as step height between the substrate and the deposited nanofiber web surface. The measurement was performed using a scan speed of 0.05 mm/s, and stylus contact force of  $5 \times 10^{-5}$  kg.

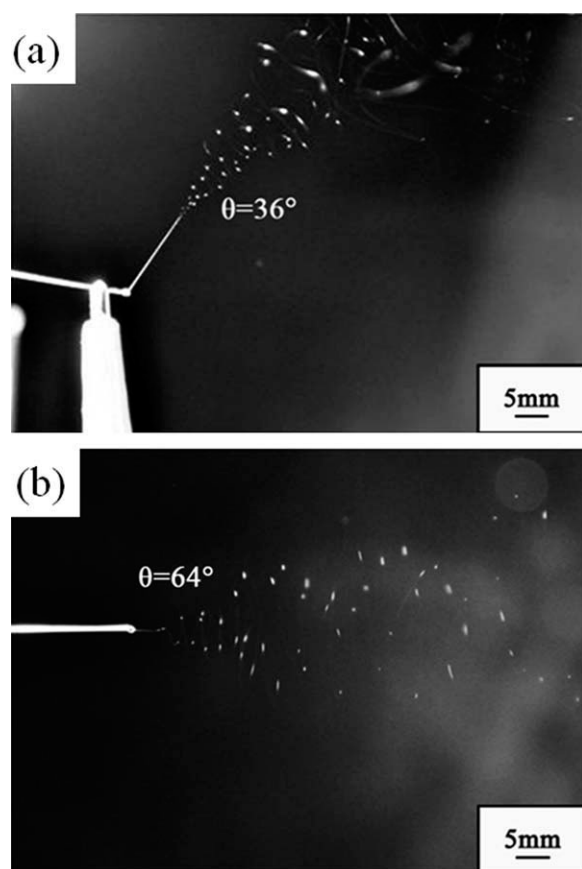
## RESULTS

### Effects of electrical polarity on the jet movement and deposited web configuration

Figure 3(a) shows the jet movement of a typical spinneret charging system electrospun under the following conditions: applied voltage of 20 kV, working distance of 18 cm, and flow rate of 0.008 mL/min. As the electrostatic field applied, a charged jet flow was ejected upward from the tip of the Taylor cone and followed by whipping occurred at the end of jetting. The upward jet flow resulted from the gripped position and direction of the charging clip. As the solvent evaporated and the charge density increased, the whipping amplitude was enlarged



**Figure 2** Typical image of jet movement during electrospinning process.

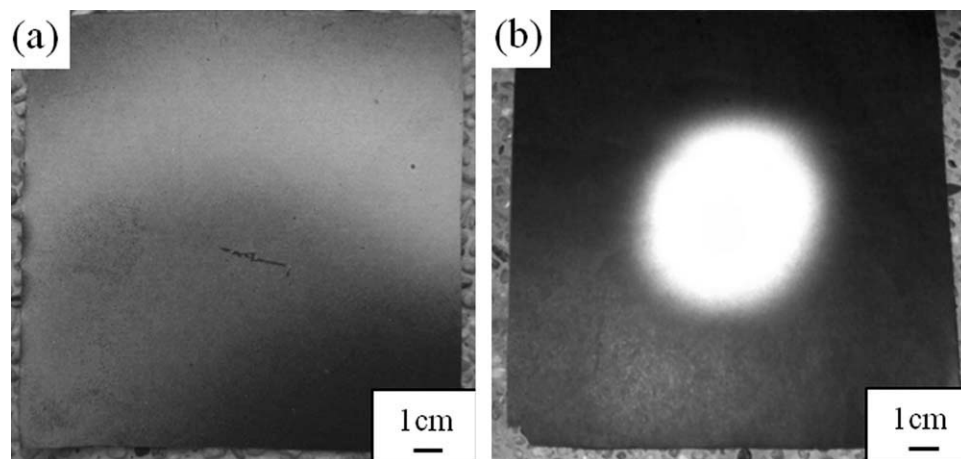


**Figure 3** Images of jet movement for (a) spinneret charging system, (b) collector charging system, at electrospinning conditions: applied voltage: 20 kV, working distance: 18 cm, flow rate: 0.008 mL/min, RH%: 40% (Electronegative charger).

gradually and getting irregular. However, we still can find an inverted whipping cone with a whipping angle of  $36^\circ$ . Figure 3(b) shows the jet movement of a typical collector charging system at the same electrospinning conditions. When the collector









was electronegatively charged, an induced electropositive charging liquid drop was ejected straightly from the tip of the Taylor cone and followed by whipping occurred at the end of jetting. A slightly downward jet flow is observed owing to gravity. It is found that the jet movement process: from base via jet, whipping to collection can be applied to both charging systems. However, some quantitative differences existed between the two charging systems such as the straight jet length, whipping angle, and pitch of whipping loop. It is clear that the straight jet length in the collector charging system (3 mm) is much shorter than that in the spinneret charging system (13 mm). The results suggest that the jetting velocity and effective charge density of the polymer jet which response to the repulsive force in the spinneret charging system are higher than that of the collector charging system. When high voltage is applied to the spinneret, the polymer solution is getting much more charge compared to when high voltage is applied to the collector. For the whipping angle, it is  $64^\circ$  for the collector charging system and  $36^\circ$  for the spinneret charging system. The polymer is less charged in the collector charging system, leading to less acceleration owing to the electric field, results shorter straight jet path and a wider whipping cone. The pitch of whipping loop is 2.05 mm for the collector charging system and 1.14 mm for the spinneret charging system. The result is relative to higher jetting velocity in the spinneret charging system.

Figure 4 shows the deposited web configurations on the collector in spinneret charging system [Fig. 4(a)] and collector charging system [Fig. 4(b)]. In the spinneret charging system, the fibers tended to deposit randomly over the collector and formed a large spreading fiber web as shown in Figure 4(a). This deposited fiber web is rough and not well-distributed. In contrast, a confined and more compact fiber web



**Figure 4** Typical deposited web configuration for (a) spinneret charging system, (b) collector charging system, at electrospinning conditions: applied voltage: 20 kV, working distance: 18 cm, flow rate: 0.008 mL/min, RH%: 40% (Electronegative charger).

**TABLE I**  
**Effects of Applied Voltages on Electrospinning Behavior and Fiber Productivity in the Spinneret Charging System (Electronegative Charger)**

Applied voltage (kV)	Straight jet length (mm)	Whipping angle (°)	Pitch of whipping loop (mm)	Fiber diameter (nm)	Fiber productivity (mg/min)	Taylor cone
5	11.3 ± 0.84	48 ± 3	2.41 ± 0.19	327 ± 28	0.21	
10	12.11 ± 0.53	40 ± 1	2.59 ± 0.42	308 ± 28	0.31	
15	12.44 ± 0.51	38 ± 2	1.14 ± 0.18	286 ± 26	0.39	
20	13.03 ± 0.55	36 ± 1	1.14 ± 0.25	299 ± 23	0.46	
25	14.46 ± 0.87	34 ± 1	1.03 ± 0.16	291 ± 69	0.48	
30	NA	33 ± 1	0.88 ± 0.11	337 ± 43	0.55	
35	NA	34 ± 1	0.81 ± 0.04	328 ± 73	0.55	
40	NA	34 ± 1	0.67 ± 0.09	317 ± 108	0.57	

Spinneret charging system, working distance: 18 cm, flow rate: 0.008 mL/min, RH%: 40%

deposition with circular shape in the collector charging system was observed and shown in Figure 4(b). This deposited fiber web looks even, well-distributed, and is centralized around the charged point of the collector. This means that the fiber web of collector charging system is more compact than the spinneret charging system. The results demonstrated that the electrostatic polarity strongly influences the electrospinning behavior and web configuration. It is believed that large whipping angle and short straight jet length shall contribute to thinning down the fiber and will be examined next.

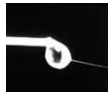

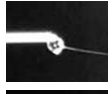

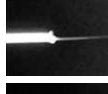
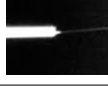
#### Effects of electrical voltage on the electrospinning behavior

In electrospinning, an external electric field is used to control the charged jet. The charge applied to the jet and dissipated by the deposited nanofibers play an important role in the electrospinning process. This process is strongly controlled by the electric field, electrostatic polarity, and the type of electrical charging. Table I summarizes the results of jetting movement and fiber diameters under various electrical voltages (5–40 kV) for the spinneret charging

system, whereas Table II lists those results under various electrical voltages (15–40 kV) obtained by the collector charging system. The onset of the processing voltage for electrospinning in this study is 15 kV (electric field: 0.83 kV/cm) for collector charging system and 5 kV (electric field: 0.28 kV/cm) for spinneret charging system. That means higher electric field is required to fulfill the electrospinning process for collector charging system.

Observing the images of Taylor cone in Tables I and II, a teardrop is found at low voltages in the range of 5–15 kV in spinneret charging system and in the range of 15–25 kV in collector charging system. At low applied voltages, the ejected flux of polymer solution caused by the applied electric field was less than the extruded flux provided by the syringe pump at a constant flow rate. As a result, the droplet enlarged gradually and formed a teardrop shape accompanied with the effect of gravity. When size of the developing PVA droplet was over, the droplet spilled out and caused discontinuous electrospinning process and it resulted in reduced productivity. The droplet size shrunk with increasing of applied voltage. At high voltage (25–40 kV in spinneret charging system and 35–40 kV in collector

**TABLE II**  
**Effects of Applied Voltages on Electrospinning Behavior and Fiber Productivity in the Collector Charging System (Electronegative Charger)**

Applied voltage (kV)	Straight jet length (mm)	Whipping angle (°)	Pitch of whipping loop (mm)	Fiber diameter (nm)	Fiber productivity (mg/min)	Taylor cone
15	3.15 ± 0.41	60 ± 5	3.34 ± 0.50	242 ± 15	0.58	
20	3.06 ± 0.58	64 ± 3	2.05 ± 0.14	240 ± 25	0.74	
25	3.58 ± 0.24	60 ± 1	1.85 ± 0.21	209 ± 35	0.82	
30	5.76 ± 0.15	50 ± 1	1.13 ± 0.06	274 ± 32	0.84	
35	6.03 ± 0.77	44 ± 2	1.10 ± 0.15	244 ± 44	0.92	
40	NA	33 ± 2	1.23 ± 0.08	264 ± 31	0.84	

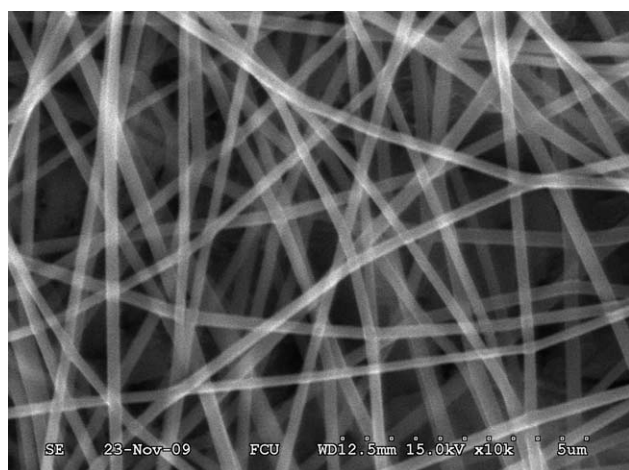
Collector charging system, working distance: 18 cm, flow rate: 0.008 mL/min, RH%: 40%

charging system), the great amount of charges accelerated the jet movement and more volume of solution was drawn from the tip of the needle. Therefore, the Taylor cone receded into the needle owing to the drawing of the solution to the collector being faster than the supply from the source. The electrospinning process at high electric field resulted in less stable Taylor cone formation and jetting instability. Therefore, optimal electrospinning condition occurs when equilibrium of the flow rate and electrostatic extraction force is accomplished.

Observation on the electrospinning jet in both systems, the straight jet length increased with voltage as summarized in Tables I and II. The length increased from 11.3 to 14.46 mm in the spinneret charging system, and from 3.06 to 6.03 mm in the collector charging system. This result fits the description of Reneker's modeling<sup>13</sup> that the straight jet length increases with the applied voltage. At high voltage, the straight jet was quit unstable and the length varied with the process of electrospinning. We referred instable straight jet length as "NA." This unstable jet is related to the withdrawal of Taylor cone (droplet) owing to the extruded flux being insufficient for fully supplying the ejecting flux requirement. It is noteworthy that the straight jet length in the spinneret charging system was much longer in comparison to the collector charging system. That is, the electrostatic polarity should also be considered as an important factor that affects the straight jet length and the jet movement.

Tables I and II summarize the results of whipping angle observed in the experiments and it decreased with increasing voltage in both systems: from 48 to 33° in the spinneret charging system and 64 to 33° in the collector charging system. The pitch of whipping loop decreased from 2.59 to 0.67 (mm/loop) in the spinneret charging system, and from 3.34 to 1.1 (mm/loop) in the collector charging system. The value of whipping angle and pitch of whipping loop in the spinneret charging system were less than that in the collector charging system.

Figure 5 shows a typical scanning electron micrograph of PVA nanofiber web produced in the spinneret charging system. There is no visible morphological difference except the fiber diameter at various applied voltages for the two different charging systems. The fiber diameter was determined and summarized in Tables I and II. Checking on the fiber diameter results, we can find that electrospun fibers obtained in the collector charging system were finer than those in the spinneret charging system. The optimal voltage to obtain the finest nanofiber in the spinneret charging system was 15 kV, with fiber diameter of 286 nm, whereas in the collector charging system it was 25 kV, with fiber diameter of 209 nm. As we know, the instability region is the primary cause for the rapid decrease of the fiber diameter and the large stretch ratio obtained in electrospun nanofibers.<sup>18</sup> The whipping path can be estimated based on the results of straight jet length, whipping angle, and pitch of



**Figure 5** Scanning electron micrograph shows a typical electrospun PVA nanofiber web for collector charging system, at electrospinning conditions: applied voltage: 15 kV, working distance: 18 cm, flow rate: 0.008 mL/min, RH%: 40% (Electronegative charger).

whipping loop. The collector charging system with longer whipping path may result in thinning down the electrospun fiber. In addition, the fiber diameter decreased with increasing applied voltage in both charging systems. However, when instable jet movement occurred at higher voltage, the fiber diameter and the standard deviation of fiber diameter became larger. Therefore, optimal electrospinning conditions occurred at 15–20 kV for spinneret charging system and 25–30 kV for collector charging system and resulted in finer fiber diameter.

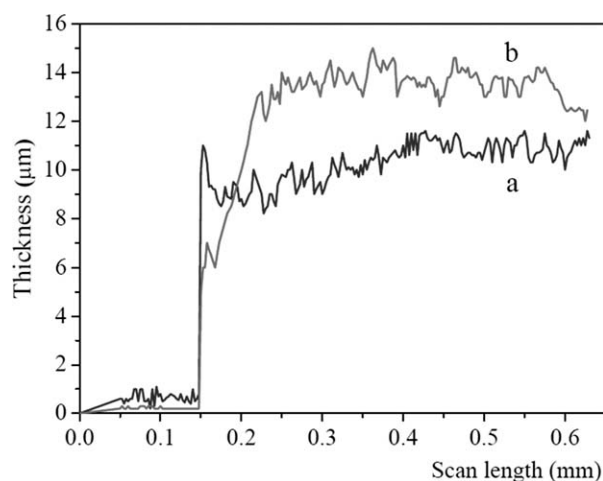
To evaluate the electrospinning productivity, fibers were electrospun for 30 min under various applied voltages. The deposited fibers within area of  $15 \times 15 \text{ cm}^2$  were weighted. This weighted value divided by the electrospinning time was regarded as electrospinning productivity and listed in Tables I and II. The resulted productivity for the collector charging system is larger than that of the spinneret charging system. When electrical voltage ranges from 5 to 15 kV for the spinneret charging system and 15 to 25 kV for the collector charging system, the electrostatic forces are not strong enough to eject all the polymer solutions which were pumped out constantly. Some polymer solutions spilled out and resulted in a reduction of net weight. However, the productivity increased as the electrical voltage increased and tended to a constant mass (0.55 mg/min for the spinneret charging system and 0.84 mg/min for the collector charging system).

Based on the abovementioned fiber productivity results, nanofiber webs prepared at the optimal electrospinning conditions of the two charging systems with similar net weight were compensated by the duration of electrospinning. The thickness of the deposited nanofiber web was measured by a stylus

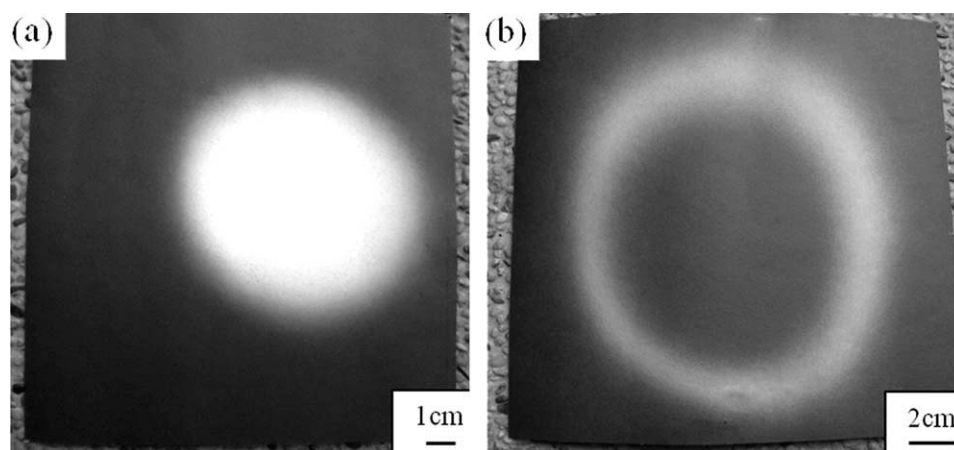
contact type machine as shown in Figure 6. The average thicknesses are approximately 14 and 11  $\mu\text{m}$  for the collector charging system and spinneret charging system, respectively. The results confirm that the fiber web of collector charging system is more compact than the spinneret charging system.

## DISCUSSION

Based on the above-presented results, it is observed that the collector charging system has many merits compared to spinneret charging system such as homogeneously distributed and compact fiber web, finer fiber diameter, and higher productivity. The same kind of study has been conducted by Kilic et al.<sup>35</sup> with positive electrical charger. But Kilic et al.<sup>35</sup> observed the similar merits in the spinneret charging system. To clarify this paradox, a positive electricity power supply (Apollo-P60, Taiwell, Taiwan) was utilized to perform the inverse polarity experiments. As shown in Figure 7(a), a confined, compact, and thicker fiber deposited configuration was observed in the spinneret charging system. This confined nanofiber deposited configuration was similar to that in the collector charging system by using electronegative charger, whereas an uneven circular shape fiber deposited configuration was found in the collector charging system [Fig. 7(b)]. The morphological feature of the electrospun nanofiber obtained by using the electropositive charger has no visible difference to that of the electronegative one as shown in Figure 5. The results for fiber diameter and productivity obtained by different charging systems at various applied voltages are summarized in



**Figure 6** Thickness profile of the deposited nanofiber web for (a) spinneret charging system at electrospinning conditions: applied voltage: 15 kV, working distance: 18 cm, flow rate: 0.008 mL/min, RH%: 40%, (b) collector charging system at electrospinning conditions: applied voltage: 25 kV, working distance: 18 cm, flow rate: 0.008 mL/min, RH%: 40% (Electronegative charger).



**Figure 7** Typical deposited web configuration by using electropositive charger for (a) spinneret charging system, (b) collector charging system, at electrospinning conditions: applied voltage: 30 kV, working distance: 18 cm, flow rate: 0.008 mL/min, RH%: 40%.

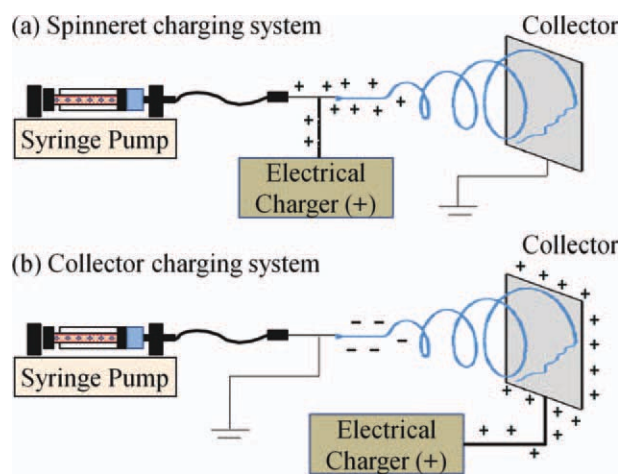
Table III. In the spinneret charging system, the obtained fiber diameter ranged from 247 to 276 nm, whereas it was from 264 to 346 nm for the collector charging system. The nanofiber productivity was 0.9 mg/min for the spinneret system and 0.2 mg/min for the collector charging system. The heavy deposited fiber webs in the spinneret system indicated a higher efficient productivity. The results obtained by electropositive system were similar to the findings of Kilic et al.<sup>35</sup> but seemed contrary to the results by electronegative system. It is, therefore, to deduce that the properties and behavior of electrospun PVA nanofiber webs were strongly influenced by the electrostatic polarized direction and the type of electrical charger.

It is noteworthy that, when collector charged negatively (collector charging system), electropositive charges were induced and accumulated on the PVA spinning jet [Fig. 1(b)]. This positively charged spin-

ning jet can be achieved directly in the spinneret charging system by using electropositive charger [Fig. 8(a)]. Similarly, negatively charged spinning jet can be achieved directly in the spinneret charging system by using electronegative charger [Fig. 1(a)] or in the collector charging system by using electropositive charger [Fig. 8(b)]. It is observed that a better electrospinning performance like fine fiber diameter, compact fiber web configuration, and higher productivity was obtained in the collector charging system by using electronegative charger and in the spinneret charging system by using electropositive charger. Therefore, we conclude that PVA electrospinning jet with electropositive charges has better electrospinning behavior and performances. That is, PVA solution is easier to be ejected and whipped under electropositive charging. This finding is an

**TABLE III**  
Effects of Applied Voltages on the Electrospinning Fiber Diameter and Productivity for Differently Polarized Charging Systems Charged by Electropositive Power Supply

Applied voltages (kV)	Fiber diameters (nm)		Fiber productivity (mg/min)	
	Spinneret charging system	Collector charging system	Spinneret charging system	Collector charging system
5	262 ± 53	NA	0.27	NA
10	276 ± 40	NA	0.34	NA
15	272 ± 38	328 ± 55	0.29	0.11
20	268 ± 45	290 ± 47	0.37	0.08
25	265 ± 38	284 ± 67	0.88	0.18
30	247 ± 34	264 ± 43	0.82	0.21
35	258 ± 45	346 ± 65	0.91	0.15
40	259 ± 34	282 ± 60	0.90	0.19



**Figure 8** Schematic diagram of two electrospinning apparatus (a) spinneret charging system and (b) collector charging system (electropositive charger). [Color figure can be viewed in the online issue, which is available at [www.interscience.wiley.com](http://www.interscience.wiley.com).]



important guideline for the designing of electrospinning device. For example, it is better to spin the PVA nanofibers by using spinneret charging system with electropositive charger for the electrospinning device with rotating collector. The collector charging system with electronegative charger is not recommended, because directly charging the collector would damage the rotating motor or other electronic controller. For the spinneret electropositive charging system, a grounded collector is easier to couple with some other controller or electronic devices. Besides, for a melt electrospinning machine with conventional extruder, it is recommended to use the collector charging system to prevent the extruder from being damaged. Then, a suitable electrical charger is selected to adapt the polymer melt.

Based on the above discussion, we know that every polymer solution or polymer melts have their own applicable electric characteristic for electrospinning.<sup>36</sup> This electric preference may be attributed to the polarity of polymer and solvent material and warrant further investigations.

### CONCLUSION

Effects of electrostatic polarity and the use of electrical charger on the electrospinning behavior were studied by two inverse polarity electrospinning systems. The results showed that the collector charging system displayed shorter straight jet length, larger whipping angle, compact and thicker fiber deposited configuration, higher fiber productivity, and finer fiber diameter (electronegative power system). Higher electrical force is required to fulfill the electrospinning process for collector charging system with electronegative charger. At higher applied voltages, the Taylor cone receded into the needle and the straight jet segment became unstable and caused an increase in fiber diameter and its standard deviation. The optimal electrospinning condition occurs when the equilibrium of flow rate and electrostatic extraction force is accomplished. The optimal voltage for obtaining the finest electrospun nanofiber was 25 kV for electronegative collector charging system (fiber diameter, 209 nm) and 30 kV for electropositive spinneret charging system (fiber diameter, 247 nm).

PVA solution jet is easier to be ejected and whipped under electropositive charging. The PVA electrospinning jet with electropositive charges exhibited better electrospinning behavior and performances. The spinning jet with electropositive charges can be achieved either in the spinneret charging system by using electropositive charger or in the collector charging system by using electronegative charger. This finding is an important guideline for the designing of electrospinning device. Every polymer solution or polymer melts have their appli-

cable electric characteristic for electrospinning which may be attributed to the polarity of polymer and solvent material and warrant further investigations.

### References

- Ramakrishna, S.; Fujihara, K.; Teo, W. E.; Lim, T. C.; Ma, Z. An Introduction to Electrospinning and Nanofibers; World Scientific: Singapore, 2005.
- Wang, C.; Chien, H. S.; Hsu, C. H.; Wang, Y. C.; Wang, C. T.; Lu, H. A. *Macromolecules* 2007, 40, 7973.
- Dersch, R.; Steinhart, M.; Boudriot, U.; Greiner, A.; Wendorff, J. H. *Polym Adv Technol* 2005, 16, 276.
- Huang, Z. M.; Zhang, Y. Z.; Kotakic, M.; Ramakrishna, S. *Compos Sci Technol* 2003, 63, 2223.
- Sun, K.; Li, Z. H. *Express Polym Lett* 2011, 5, 342.
- Nagy, Z. K.; Nyul, K.; Wagner, I.; Molnar, K.; Marosi, G. *Express Polym Lett* 2010, 4, 763.
- Feng, C.; Khulbe, K. C.; Matsuura, T. *J Appl Polym Sci* 2010, 115, 756.
- Deitzel, J. M.; Kleinmeyer, J.; Harris, D.; Beck Tan, N. C. *Polymer* 2001, 42, 261.
- Saville, D. A. *Phys Fluids* 1971, 14, 1095.
- Heikkilä, P.; Harlin, A. *Eur Polym J* 2008, 44, 3067.
- Reneker, D. H.; Yarin, A. L. *Polymer* 2008, 49, 2387.
- Yarin, A. L.; Koombhongse, S.; Reneker, D. H. *J Appl Phys* 2001, 90, 4836.
- Reneker, D. H.; Yarin, A. L.; Fong, H.; Koombhongse, S. *J Appl Phys* 2000, 87, 4531.
- Tong, H.-W.; Wang, M. *J Appl Polym Sci* 2011, 120, 1694.
- Yarin, A. L.; Koombhongse, S.; Reneker, D. H. *J Appl Phys* 2001, 89, 3018.
- Fong, H.; Chun, I.; Reneker, D. H. *Polymer* 1999, 40, 4585.
- He, J. H.; Wu, Y.; Zuo, W. W. *Polymer* 2005, 46, 12637.
- Shin, Y. M.; Hohman, M. M.; Brenner, M. P.; Rutledge, G. C. *Polymer* 2001, 42, 9955.
- Ding, B.; Kimura, E.; Sato, T.; Fujita, S.; Shiratori, S. *Polymer* 2004, 45, 1895.
- Theron, S. A.; Yarin, A. L.; Zussman, E.; Kroll, E. *Polymer* 2005, 46, 2889.
- Kim, G. H.; Cho, Y. S.; Kim, W. D. *Eur Polym J* 2006, 42, 2031.
- Holzmeister, A.; Rudisile, M.; Greiner, A.; Wendorff, J. H. *Eur Polym J* 2007, 43, 4859.
- Yarin, A. L.; Zussman, E. *Polymer* 2004, 45, 2977.
- Moon, S. C.; Choi, J. K.; Farris, R. J. *J Appl Polym Sci* 2008, 109, 691.
- You, Y.; Lee, S. J.; Min, B.; Park, W. H. *J Appl Polym Sci* 2006, 99, 1214.
- Katta, P.; Alessandro, M.; Ramsier, R. D.; Chase, G. G. *Nano Lett* 2004, 4, 2215.
- Sundaray, B.; Subramanian, V.; Natarajan, T. S.; Xiang, R. Z.; Chang, C. C.; Fann, W. S. *Appl Phys Lett* 2004, 84, 1222.
- Theron, A.; Zussman, E.; Yarin, A. L. *Nanotechnology* 2001, 12, 384.
- Bazbouz, M. B.; Stylios, G. K. *J Appl Polym Sci* 2008, 107, 3023.
- Teo, W. E.; Kotaki, M.; Mo, X. M.; Ramakrishna, S. *Nanotechnology* 2005, 16, 918.
- Deitzel, J. M.; Kleinmeyer, J. D.; Hirvonen, J. K.; Beck Tan, N. C. *Polymer* 2001, 42, 8163.
- Li, D.; Ouyang, G.; McCann, J. T.; Xia, Y. N. *Nano Lett* 2005, 5, 913.
- Bazbouz, M. B.; Stylios, G. K. *Eur Polym J* 2008, 44, 1.
- Chang, Z. J.; Zhao, X.; Zhang, Q. H.; Chen, D. J. *Express Polym Lett* 2010, 4, 47.
- Kilic, A.; Oruc, F.; Demir, A. *Text Res J* 2008, 78, 532.
- Eda, G.; Liu, J.; Shivkumar, S. *Eur Polym J* 2007, 43, 1154.